(NASA-CR-173847) STUDY OF DOUBLE WALL PANELS FOR USE IN PROPELLER DRIVEN AIRCRAFT (Purdue Univ.) 24 p HC A02/MF A01 CSCL 20A N84-32116

Unclas
G3/71 01015

RAY W. HERRICK LABORATORIES

A Graduate Research Facility of The School of Mechanical Engineering

Purdue University

West Lafayette, Indiana 47907

STUDY OF METHODS TO PREDICT AND MEASURE THE TRANSMISSION OF SOUND THROUGH THE WALLS OF LIGHT AIRCRAFT

Research Contract #0226-52-1288

STUDY OF DOUBLE WALL PANELS FOR USE IN PROPELLER DRIVEN AIRCRAFT

Sponsored by

NASA
Hampton, VA 22365

Report No. # 0226-10 HL 84-13

Submitted by:

Mahabir Atwal, Visiting Scholar
Robert Bernhard, Principal Investigator

Approved by:

Raymond Cohen, Director
Ray W. Herrick Laboratories

May 1984

STUDY OF DOUBLE WALL PANELS FOR USE IN PROPELLER DRIVEN AIRCRAFT

1. INTRODUCTION

Recently there has been a renewed interest in the prediction and control of interior noise in propeller-driven aircraft. This interest has arisen in part by the efforts to develop high speed advanced turboprop aircraft. Propeller-driven aircrafts have historically exhibited high levels of interior noise at the blade passage frequency and its harmonics, which is transmitted through the fuselage sidewall structure. The information available in the literature and ongoing research programs indicates that noise in many such aircrafts, exceeds acceptable comfort limits and also the maximum noise intensity occurs at low frequencies. Since most type of acoustic absorption materials used in aircraft constructions are not very effective at low frequencies, other means of providing noise attenuation with minimum of mass penalty at these frequencies need to be established.

In order to reduce the cabin noise significantly, improved sidewall attenuation and absorption within the cabin are expected to be required in addition to the reduction of source noise levels. In this report method of interior noise control by means of efficient sidewall attenuation is discussed.

One way of increasing the attenuation or the transmission loss of the cabin sidewall panels, is to use two panels separated by an air gap. Such a double panel is much more effective than a

single panel of twice the mass per unit area. This is due to impedance 'mismatch' experienced by the sound wave. Whenever there exists a 'mismatch', a reflected wave is set up which will start at the receiving end and travel towards the source. Greater the impedance 'mismatch', higher the reflected sound wave intensity.

This report describes experimental and theoretical studies of transmission loss of two types of double panels which can be used in propeller driven aircrafts, without any mass penalty but with considerably higher transmission loss.

2. MEASUREMENT OF TRANSMISSION LOSS

To rate the sound insulating properties of a wall or a panel, the difference between incident intensity level and transmitted intensity level is desired. This difference is called the transmission loss. The most widely used method for the measurements of the transmission loss of panels is the transmission suite method. The two microphone sound intensity method is also becoming popular and the transmission loss of different types of panels have been successfully measured by several researchers at Herrick Laboratories using the intensity technique. In this study, the intensity method was used to measure the transmission loss of the panels under investigation.

Experiments were conducted to measure the diffuse field intensity in the reverberation room and the acoustic intensity

transmitted by the panel. The two walls of the double panel were bolted to the inside and the outside of a frame in an opening of one wall in the reverberation room. The panel edge conditions were intended to be fully fixed and the edges between the panel and the frame, as well as the edges between the frame and the wall of the opening were fully sealed with modeling clay to minimize any leaks. The diffuse field inside the reverberation room was produced by two Altec speaker positioned at the two rear corners of the room.

The incident intensity was assumed to be given by the diffuse field intensity

$$I_i = \frac{p_{rms}^2}{4\rho C} \qquad (1)$$

where p_{rms}^2 is the space averaged rms sound pressure measured in the reverberation chamber, ρ is the density of air and C is the speed of sound in air. As such, the sound pressure was measured using half-inch microphone rotating on a boom. Measurements were taken at four different positions in the room and the average value of these four measurements was used to calculate the diffuse field incident intensity.

The transmitted intensity was measured using two half-inch phase-matched microphones, arranged face-to-face. Microphone spacing of 50 mm and 12 mm were used, such that the range of frequency of interest (63 Hz - 5 kHz) could be covered. The output signals from the microphones was passed through measuring

amplifiers and anti-aliasing filters before being fed to the fast fourier transformer (FFT), where the data was recorded as 2 Hz narrow band for the 50 mm spacing and 10 Hz narrow band for the 12 mm spacing. With the help of a specially written fortran program it was possible to convert the data into one-third octaves, if required. The transmitted intensity for each panel was measured by sweeping the two microphone array over the exterior of each double panel of interest. Sweeping was done as close as possible to each panel and care was taken to reduce the background noise on the transmission side.

3. RESULTS

Two different type of partitions were investigated. The first type consisted of two aluminum panels with the inner space being filled with helium gas. The second type consisted of two panels with the second panel being perforated.

3.1 Effect Of Helium On Transmission Loss Of a Double Wall Panel

A major difficulty encountered in this part of the investigation was containing the helium gas between the two panels. This was overcome by designing a 'bag' similar in dimension to the spacing between the two panels which will hold the helium for a period of time required to make the measurements. This 'bag' was placed between the two panels. The 'bag' was initially filled with air and then with helium, as such, the transmitted

intensity data was taken for the two separate conditions.

Figure 1 shows the effect on the transmission loss of the double panel due to helium. As can be seen, helium increases the transmission loss of the double panel over a wide range of frequencies. This was expected because of the lower impedance of helium compared with air, as a consequence, a greater impedance mismatch.

3.2 The Effect on The Transmission Loss of a Double Panel of Perforating the Second Panel

Two different types of partitions were studied in this part of the investigation. Namely:

a. steel panel backed by a 3/16 inch pressed wood panel;

b. steel panel backed by a 3/16 inch perforated panel (3/16 inch diameter perforations every 1 inch);

c. aluminum panel backed by a 3/16 inch pressed wood panel;

d. aluminum panel backed by a 3/16 inch perforated panel (3/16 inch diameter perforations every 1 inch).

The solid and perforated panels were very similar in nature in all other respects. Figures 2 and 3 show the effect on the transmission of the double panel of perforating the second panel. As can be seen for both cases, the transmission loss of the perforated combination is higher at low frequencies, (up to about

160 Hz) the region of interest, but considerably low at frequencies higher than 160 Hz.

A simple impedance transfer model (1 based on Beranek and Work method was used to predict the transmission loss of the two perforated panel combinations in an attempt to assess the behavior of such double panels. Figures 4 and 5 show the comparison between the experimental and the predicted transmission loss. The detailed derivation of this model is discussed in the Appendix. As can be seen a fairly good fit is observed at high frequencies. The discrepancy at low frequencies is presently under investigation.

The transmission loss of perforated and unperforated single panels were also measured. Figure 6 shows the comparison between two such panels. As can be seen the transmission loss of the unperforated panel is higher throughout the frequency range.

4. REFERENCES

1. Beranek, L.L. and Work, G.A., "Sound Transmission Through Multiple Structures Containing Flexible Blankets," *J. Acoust. Soc. Am.*, Vol. 21, 419-428, 1948.

APPENDIX

A.1 Theoretical Prediction Scheme

The analytical method used to predict the transmission loss of double panel with the inner panel being perforated is summerized in this Appendix. The sound transmission geometry for this theory is given in Fig. 7, which shows the incident, reflected and transmitted plane waves at various impedance 'mismatch' boundaries. In the case of transmission of sound through a double panel, the ratio of the pressure at the back of the double panel (P_{t3}) to that in front of it (P_{i1}) is of interest. This ratio is obtained by deriving expression for the ratios $\frac{P_{i1}}{P_{t2}}$, $\frac{P_{t2}}{P_{i2}}$ and $\frac{P_{i2}}{P_{t3}}$ in terms of the various characteristic impedances and then multiplying the ratios.

$$\frac{P_{i1}}{P_{t2}} \times \frac{P_{t2}}{P_{i2}} \times \frac{P_{i2}}{P_{t3}} = \frac{P_{i1}}{P_{t3}} \qquad (2)$$

A.2 Calculation of the Pressure Ratios

a) $\frac{P_{i1}}{P_{t2}}$

The pressure (P_{i1}) and the velocity (V_{ii1}) incident on the first panel as a function of distance (x) and time (t) are respectively given by

$$P_{i1}\ (x,t) = P_o\ e^{j(\omega t-kx)} \qquad (3)$$

$$V_{i1}\ (x,t) = \frac{P_o e^{j(\omega t[kx)}}{\rho c} \qquad (4)$$

where P_o is the amplitude, ρc is the impedance of the media, ω is the radian frequency, K is the wave number and j is equal to $\sqrt{-1}$. The pressure (P_{r1}) and the velocity (V_{r1}) reflected by the first panel are respectively given by

$$P_{r1}(x,t) = RP_o e^{j(\omega t+kx)} \tag{5}$$

$$V_{ri}(x,t) = -\frac{RP_o}{\rho c} e^{J(\omega t+kx)} \tag{6}$$

where R is the reflection coefficient. Therefore, the net pressure and the velocity in front of the panel (x=0) are respectively given by

$$P_1(x,t) = P_o(HR)\ e^{j\omega t} \tag{7}$$

$$V_1(x,t) = \frac{P_o(1-R)}{\rho c} e^{j\omega t} \tag{8}$$

The impedance at the point x=0 is, therefore, equal to

$$Z = \left(\frac{1+R}{1-R}\right) \rho c \tag{9}$$

Since velocity is continuous, the ratio of the pressures on the opposite sides of the first panel are given by the impedance ratios.

$$\frac{P_{i1} + P_{r1}}{P_{t2}} = \frac{Z}{Z_1} \tag{10}$$

and at x=0,

$$\frac{P_{i1}}{P_{i1}+P_{r1}} = \frac{1}{1+R} \tag{11}$$

Hence,

$$\frac{P_{i1}}{P_{t2}} = \frac{P_{i1}}{P_{i1}+P_{r1}} \cdot \frac{P_{i1}+P_{r1}}{P_{t2}} = \frac{1}{(1+R)} \frac{Z}{Z_1} \qquad (12)$$

substituting for R from Eq. (9) yields an expression for $\frac{P_{i1}}{P_{t2}}$ in terms of the two impedances Z and Z_1.

$$\frac{P_{i1}}{P_{t2}} = \frac{Z+\rho c}{2Z_1} \qquad (13)$$

b) $\frac{P_{t2}}{P_{i2}}$

Because the velocity is continuous the ratio is given by the expression

$$\frac{P_{t2}}{P_{i2}} = \frac{Z_1}{Z_2} \qquad (14)$$

c) $\frac{P_{i2}}{P_{t3}}$

Using earlier argument

$$\frac{P_{i2}}{P_{t3}} = \frac{Z_2+\rho c}{2Z_3} \qquad (15)$$

A.3 "<u>Calculation of the Impedences</u>

a) $\underline{Z_3}$

$$Z_3 = \rho C \qquad (16)$$

b) $\underline{Z_2}$

The net force acting on the panel per unit area is given by

$$P_{i2} + P_{r2} - P_{t3} \tag{17}$$

This force is used to overcome the friction experienced by the air particles in moving through the holes (primarily due to the viscosity of the medium) and the inertia of the air mass in the channel. The effects due to resistance were investigated and were considered to be negligible and as such were ignored. Thus

$$P_{i2} + P_{r2} - P_{t3} = \rho S \Delta l \frac{\partial u}{\partial t} \tag{18}$$

where ρ is the density of air, S the total hole area per unit area of the panel and Δl is the thickness of the panel. Actually Δl is not the geometrical length of the hole (i.e., the thickness of the panel). As shown in Fig. 8 the streamline begins contracting not at the opening of the hole, but at some distance in front of it and likewise they remain contracted for some distance after leaving the hole. This behavior is taken into account by end correction (delta r). The end correction for a circular aperture with radius a and with large mutual distance between such apertures is given by

$$\delta l = \left(\frac{8}{3\Lambda}\right) a \tag{19}$$

Since this term has to be applied to both sides of the panel,

$$\Delta l = l_o + 2\delta l \tag{20}$$

where l_o is the actual thickness of the panel. Equation 18, can also be written as

$$\frac{P_{i2}-P_{r2}}{V} - \frac{P_{t3}}{V} = j\omega\rho S\Delta l \tag{21}$$

or

$$Z_2 = Z_3 + j\omega\rho S\Delta l \tag{22}$$

c) $\underline{Z_1}$

In general the total acoustic pressure at any point within the medium (Fig. 7), if the time variation is omitted is given by the super-position of the incident and the reflected waves

$$P(x) = P_{i2}\ e^{\gamma(l-x)} + P_{r2}\ e^{\gamma(l-x)} \tag{23}$$

where $\gamma = \alpha+j\beta$, is the attenuation constant and β is the phase constant. If the medium is air then $\alpha=0$. Correspondingly the particle velocity can be expressed in terms of the characteristics impedance (ρc) of the medium as

$$V(x) = \frac{P_{i2}}{\rho c}\ e^{\gamma(l-x)} - \frac{P_{r2}}{e_c}\ e^{\gamma^{(l-x)}} \tag{24}$$

Using the boundary condition

$$\frac{P(l)}{V(l)} = Z_2 \tag{25}$$

and

$$\frac{P_r}{P_i} = \frac{Z_2-\rho c}{Z_2+\rho c} \tag{26}$$

The following expression for Z_1 is obtained

$$Z_1 = \rho C \left[\frac{Z_2 \text{ Cosh}\gamma l + \rho c \text{ Sinh}\gamma l}{Z_2 \text{ Sinh}\gamma l + \rho c \text{ Cosh}\gamma l}\right] \tag{27}$$

or

$$Z_1 = \rho C \left[\text{Coth} \left[\frac{j\omega l}{c} + \Psi \right] \right] \tag{28}$$

where

$$\Psi = \text{Coth}^{-1} \left(\frac{Z_2}{\rho c}\right) \tag{29}$$

<u>Z</u>

The expression for the impedance of solid partition backed by impedance Z_1 is given by the well known expression

$$Z = j\omega M_1 + Z_1 \tag{30}$$

where M_1 is the mass per unit area of panel 1.

A.4 <u>Effect of the Angle of Incidence</u>

If the effects of the angle of incidence are also included, the following expressions for the various impedance are obtained

$$Z_3 = \frac{\rho C}{\text{Cos}\theta} \tag{31}$$

$$Z_2 = j\omega\rho S\Delta l + Z_3 \tag{32}$$

$$Z_2 = \frac{\rho c}{\text{Cos}\theta} \left[\text{Coth} \left[\frac{j\omega l \text{Cos}\theta}{C} + \Psi \right] \right] \tag{33}$$

$$\text{Coth } \Psi = \frac{Z_3 \text{Cox}\theta}{\rho c} \tag{34}$$

$$Z = j\omega M_1 + Z_1 \tag{35}$$

where θ is the angle of incidence.

4.1 Calculation of the Transmission Loss

The transmission loss of the double panel is given by

$$TL = 10 \log \left(\frac{1}{\tau}\right) \tag{36}$$

where τ is the transmissibility coefficient of the panel.

$$\tau = \frac{P_{t3}}{P_{i1}} \tag{37}$$

Substituting for the various interface pressures and impedances an expression for τ was obtained. For comparison with the results in the reverberation chamber, an average value for the transmission coefficient, $(\theta\omega)$, was calculated by integrating over the range of incidence angles using the equation

$$(\omega) = \frac{\int_0^{\theta'} \tau(\theta,\omega) \mathrm{Cos}\theta \mathrm{Sin}\theta d\theta}{\int_0^{\theta'} \mathrm{Cos}\theta \mathrm{Sin}\theta d\theta} \tag{39}$$

where θ' is the limiting value of the incidence angle θ. A value of $\theta' = 78$ was selected and integration was performed using a trapezoedal rule with 2-degree angle increments.

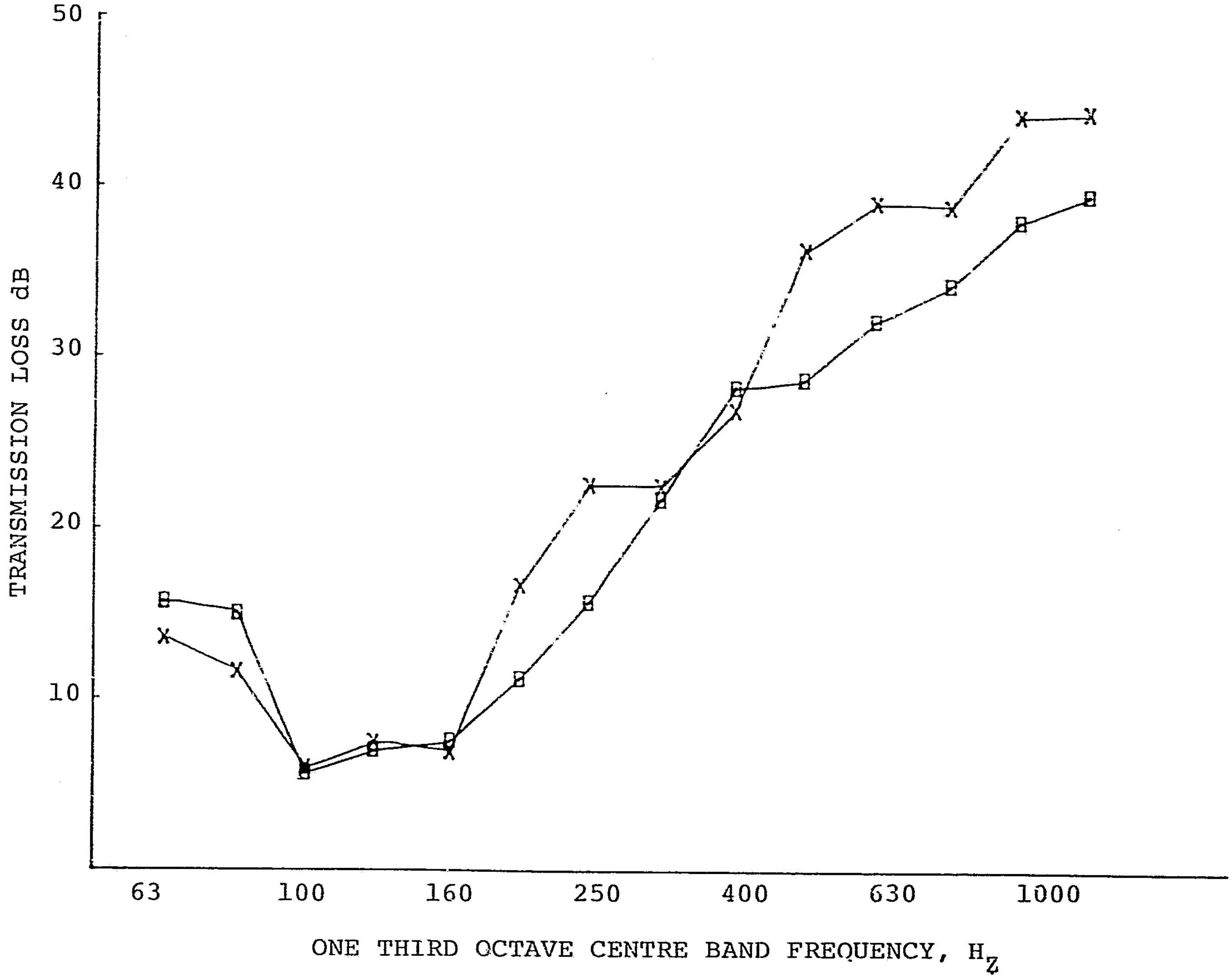

Figure 1. Effect of Helium Gas on the Transmission Loss of a Double Panel (x—x helium, —— air).

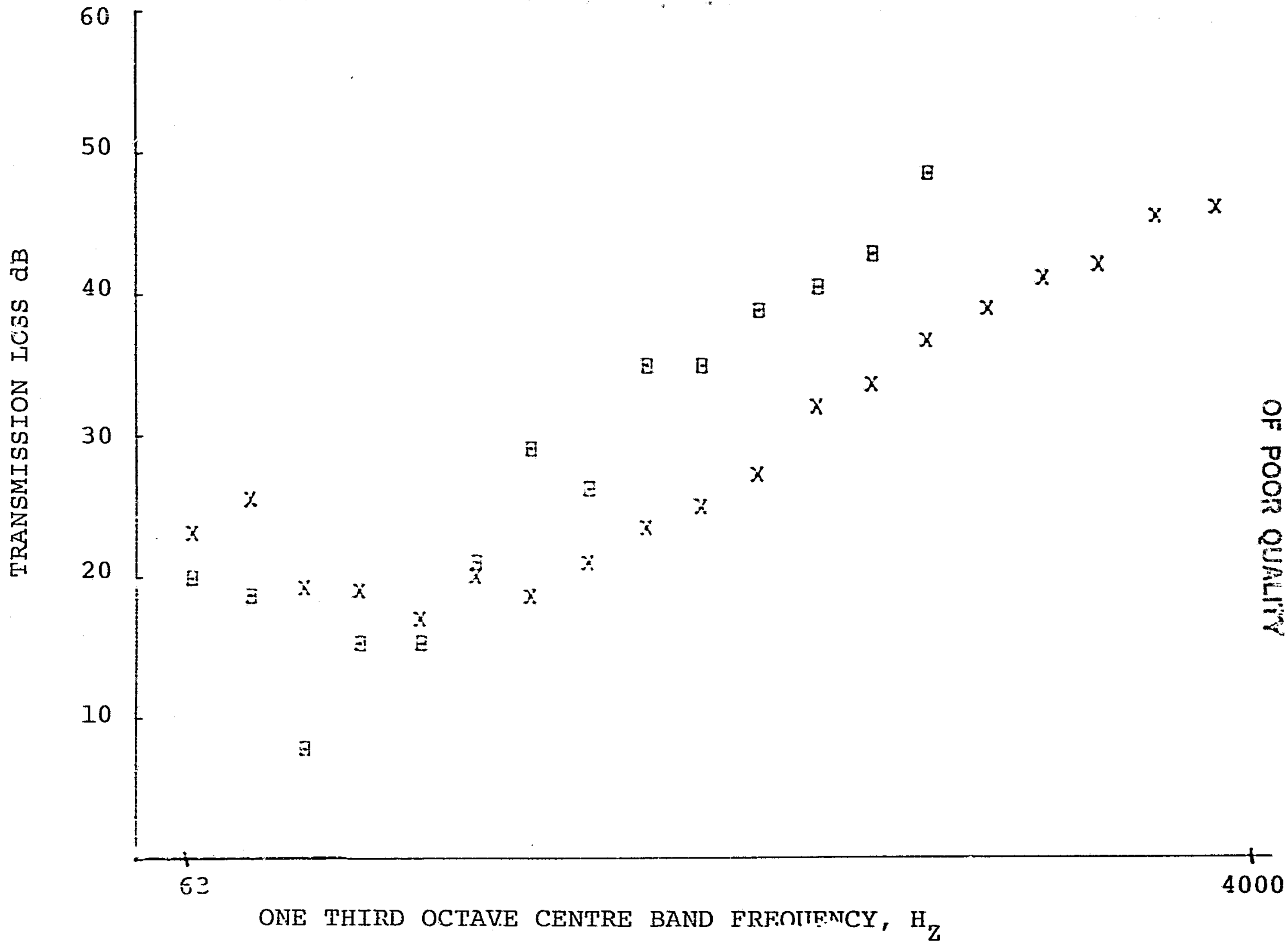

Figure 2. Effect on the transmission loss of perforating the second panel (x second panel perforated; second panel unferforated).

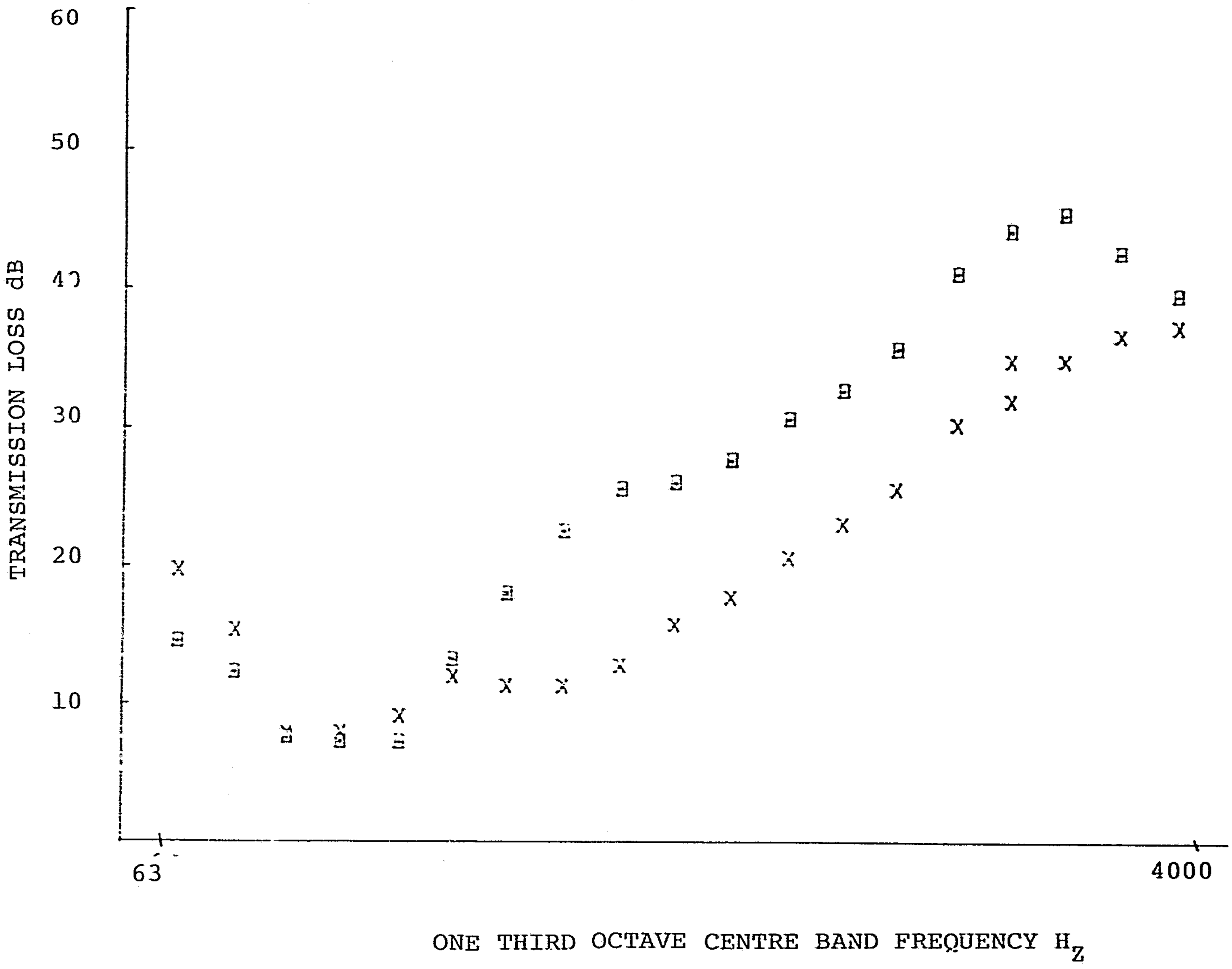

Figure 3. Effect of one transmission loss of perforating the second panel. (x second panel perforated, second panel unperforated).

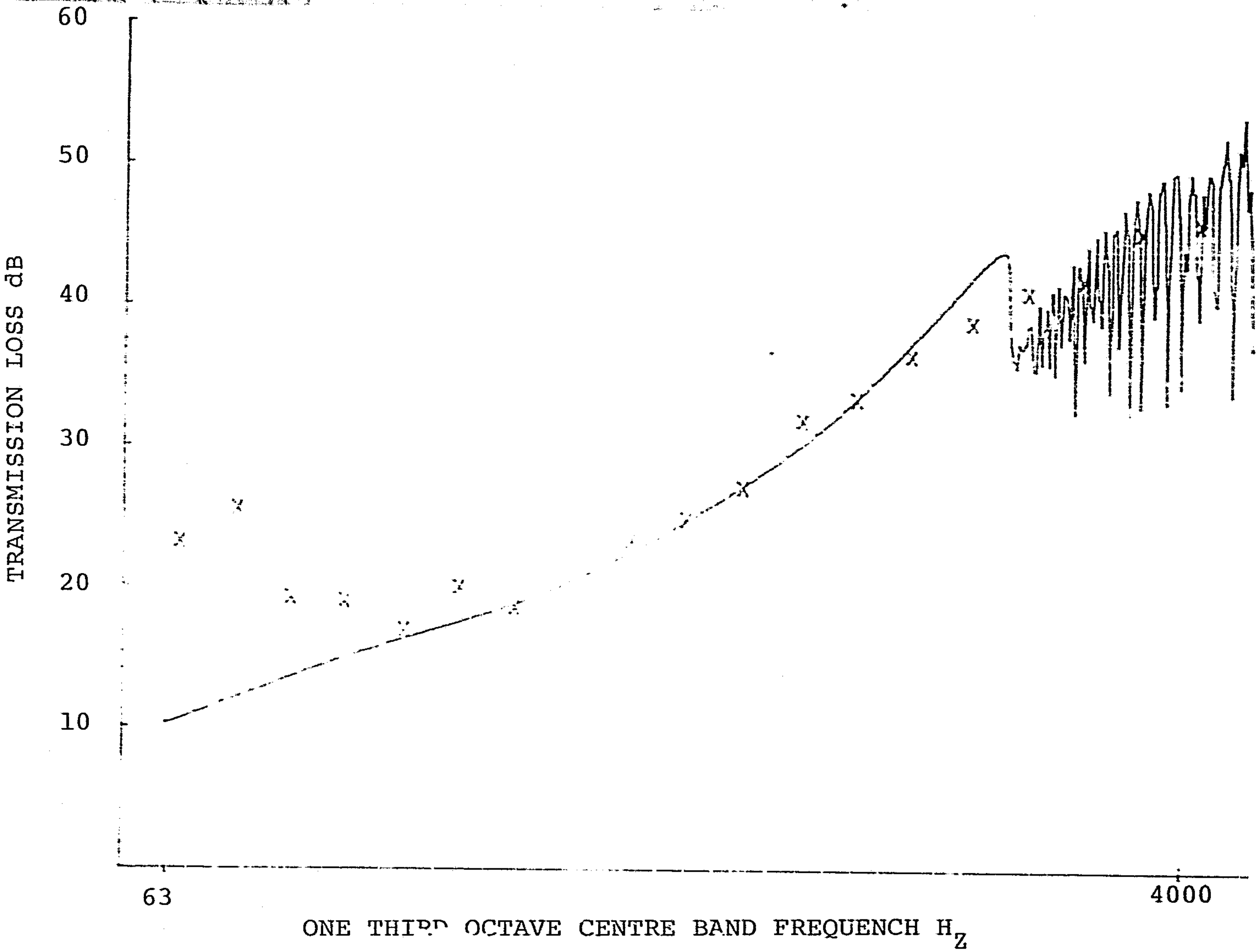

Figure 4. Comparison of experimental and theoretically predicted transmission loss (— theoretical, x experiment).

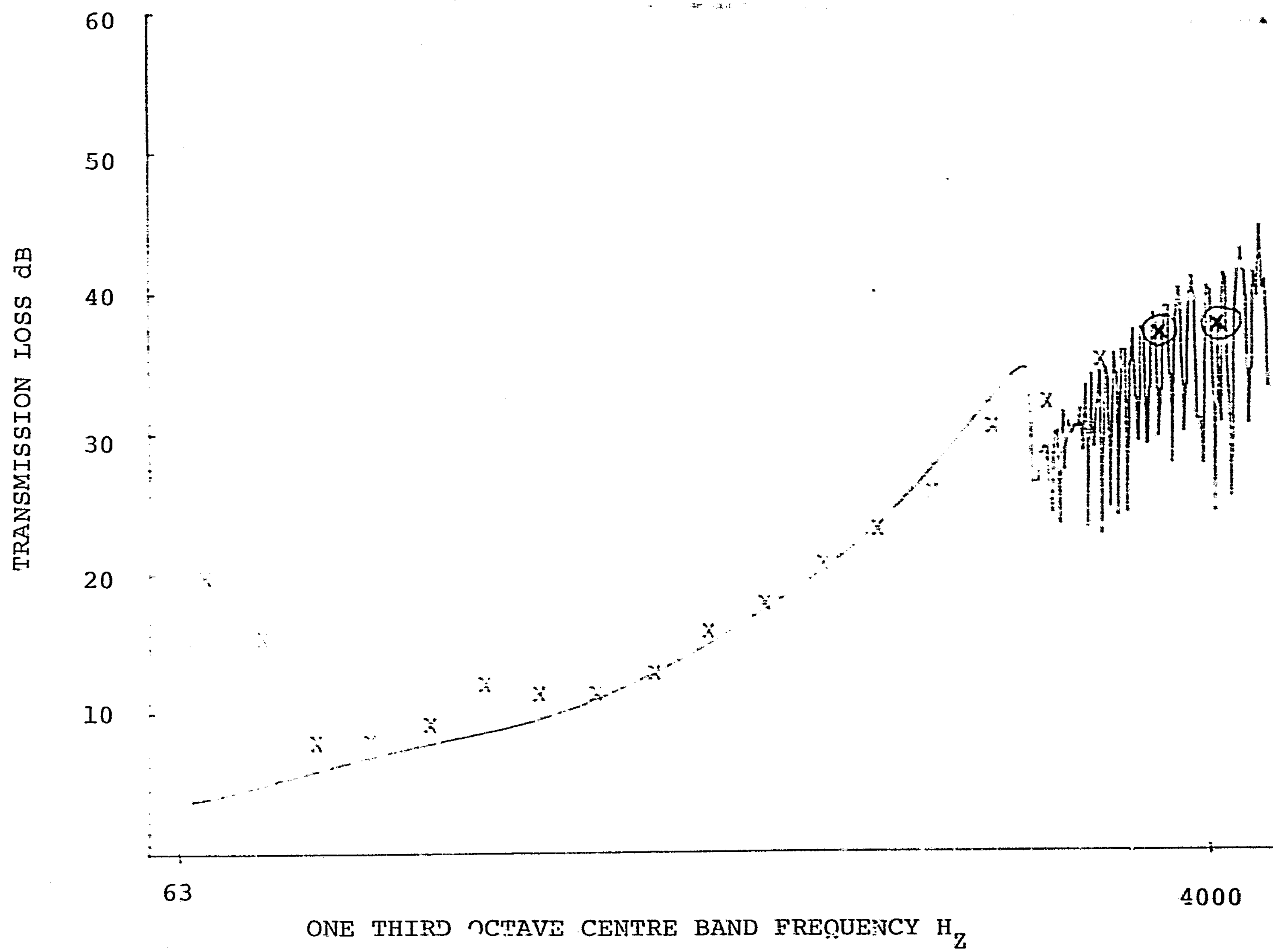

Figure 5. Comparison of Experimental and theoretical predicted transmission loss (—— theoretical, x experiment).

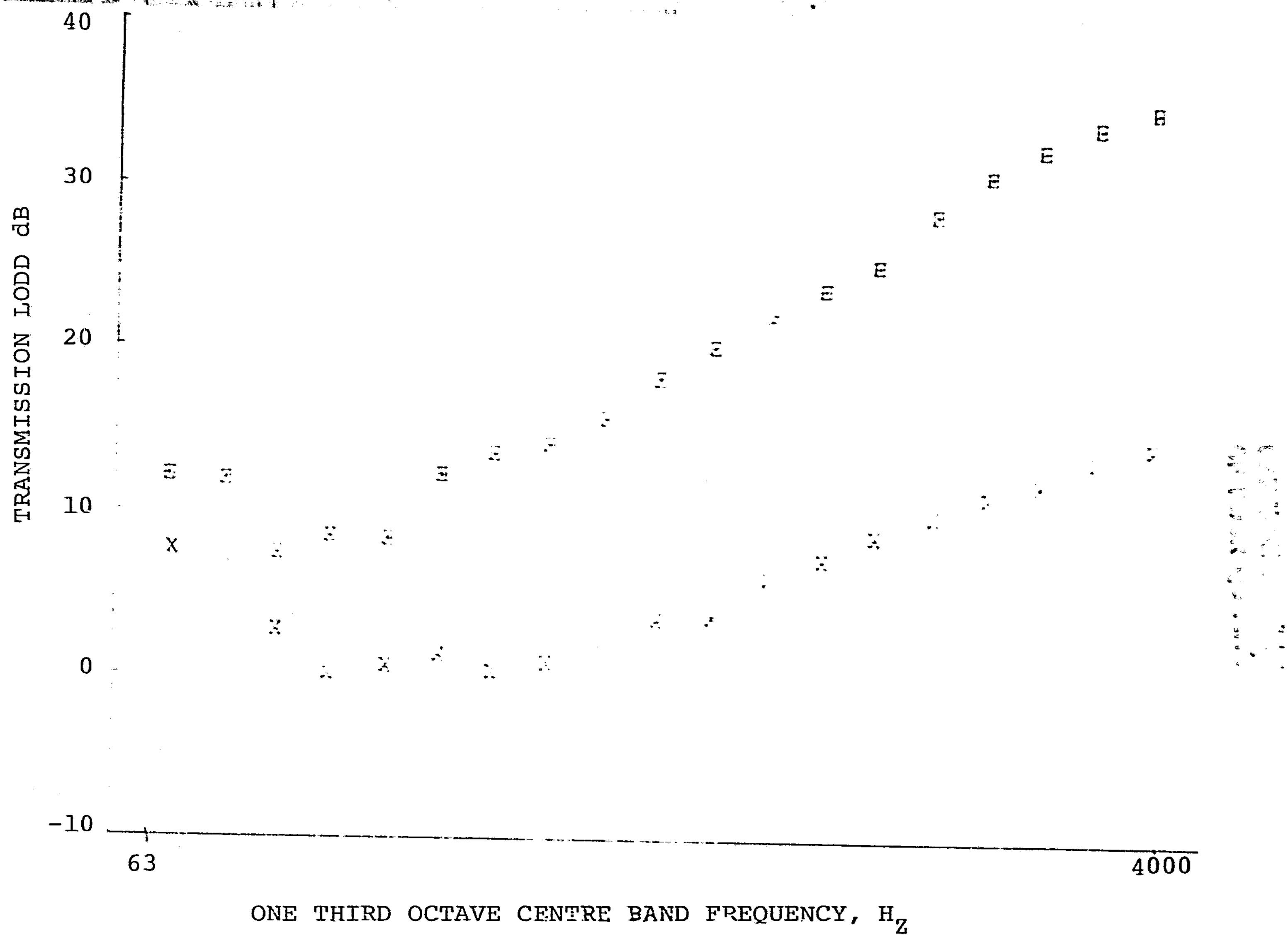

Figure 6. Comparison between the transmission loss of a perforated and unperforated single panel (unperforated, x perforated).

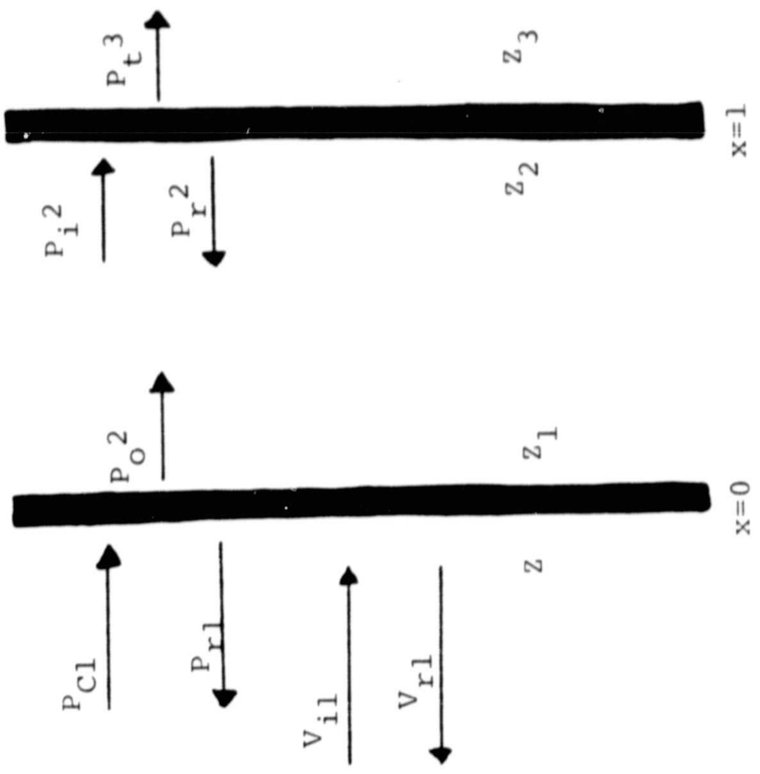

Figure 7. Double Panel Sound Transmission Geometry.

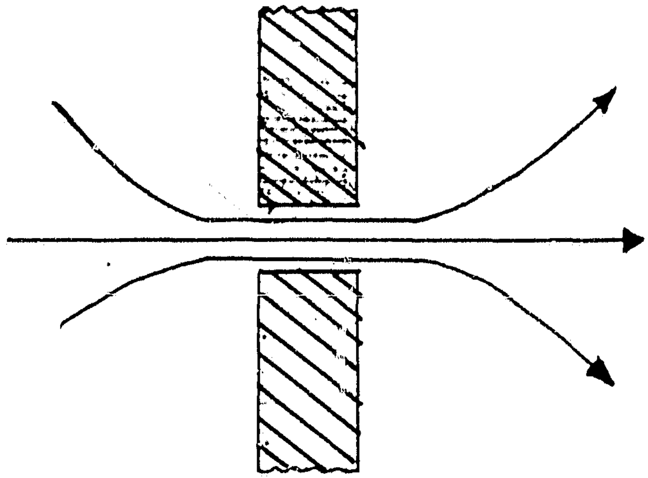

Figure 8. Air Flow Streamline Near a Ferforation.